GEUS

Report File no

17981

DANMARKS OG GRØNLANDS
GEOLOGISKE UNDERSØGELSE
RAPPORT 1996/30

Appendix No. 10

Late Permian - Early Cretaceous clay mineralogy and basin evolution in East Greenland

By Finn Surlyk and Holger Lindgreen

Geological Institute
University of Copenhagen

GEUS

Formation of Source and Reservoir Rocks in a Sequence Stratigraphic Framework, Jameson Land, East Greenland
Havniveau-kontrolleret dannelse af Kilde- og Reservoirbjergarter

Energy Research Programme 1993, Projects No. 1313/0010 & 0017
Completion Report, Appendix No. 10

Late Permian - Early Cretaceous clay mineralogy and basin evolution in East Greenland

Short title: East Greenland clay mineralogy

Holger Lindgreen and Finn Surlyk

Geological Survey of Denmark and Greenland
February 1997

LATE PERMIAN-EARLY CRETACEOUS CLAY MINERALOGY AND BASIN EVOLUTION IN EAST GREENLAND:

(Short title: East Greenland clay mineralogy)

Holger Lindgreen
Clay Mineralogical Laboratory
Geological Survey of Denmark, Thoravej 8
DK 2400 Copenhagen NV, Denmark

Finn Surlyk
Geological Institute
University of Copenhagen, Øster Voldgade 10
DK 1350 Copenhagen K, Denmark

Correspondance to:
Holger Lindgreen
Geological Survey of Denmark
Thoravej 8, DK2400 Copenhagen NV, Denmark
Phone: 45 38142913
Fax: 45 31196868
E-mail: HL@geus.dk

ABSTRACT: Clay mineralogy of Upper Permian-Lower Cretaceous mudstones from East Greenland has been investigated in order to evaluate long term trends in provenance and palaeoclimate and to detect possible volcanic events. X-ray diffraction, transmission electron microscopy and atomic force microscopy of Upper Permian-Lower Triassic mudstones show that they contain illite, chlorite, vermiculite, kaolinite, and illite-smectite (I-S) whereas the Rhaetian-Sinemurian mudstones are dominated by well-crystalline, hexagonal kaolinite. Pliensbachian-Albian mudstones contain poorly crystalline kaolinite and large amounts of I-S with ~70% illite layers. Exceptions are three Oxfordian-Kimmeridgian samples, which mainly contain I-S with 30% illite layers and two samples of Aptian mudstones with large amounts of smectite layers. Discrete clay minerals in the Upper Permian-Jurassic mudstones are largely detrital except from probably diagenetic kaolinite in the Rhaetian-Sinemurian mudstones. The smectite-rich clays are interpreted to reflect episodes of volcanic activity in the Late Jurassic and Aptian time. This is the first indication of volcanism from the Mesozoic rift basin of East Greenland. The main sediment source during Late Permian-Early Cretaceous times was weathered Precambrian and Caledonian crystalline rocks and, less importantly, older sedimentary rocks. Elevated crests of tilted fault blocks formed an additional source in Late Jurassic-Early Cretaceous times and the detrital clay minerals include illite-vermiculite and I-S ordered in IS units. The only climate-induced change is a change from chlorite, illite, vermiculite and kaolinite in Upper Permian-Lower Triassic mudstones to

kaolinite and I-S in the Jurassic mudstones. This is probably due to an increase in precipitation.

INTRODUCTION

In clays of diagenetic or lower transformation grade, variation in amount and type of discrete clay minerals can predominantly be attributed to different parent rocks, changing weathering conditions in the source area, or to clay mineral segregation in the depositional environment. This is because the main change in clay mineralogy during burial diagenesis of clays is an increase in the amount of illite layers in and degree of ordering of mixed-layer illite-smectite (I-S) (Weaver & Beck, 1971; Hower *et al.*, 1976; Pearson & Small, 1988; Lindgreen, 1991). For discrete clay minerals only small changes have been found such as formation of minor amounts of chlorite (Hurst, 1985a; Ahn & Peacor, 1985 and 1987) and possibly breakdown of detrital mica (Hower *et al.*, 1976). The importance of the source area was demonstrated for modern sediments by Milne & Early (1958) and reviewed by Weaver (1959). Recently, Hallam *et al.* (1991) suggested that a Late Jurassic change from smectite-poor sediments with abundant illite and kaolinite to sediments with abundant smectite and depleted in kaolinite, in England and France reflected a change toward more arid weathering conditions. Furthermore, they found that the change was initiated in the Oxfordian in the southern part of their study area, and first reached the northern part in the latest Volgian.

We have investigated the clay mineralogy of Upper Permian-Lower Cretaceous sediments from East Greenland in order to evaluate long-term trends in provenance and weathering and to test the hypothesis of Hallam *et al.* (1991)

concerning a climatic change in Late Jurassic or possibly earliest Cretaceous time. We have furthermore examined the samples for volcanic material, comparable to that reported from Jurassic and Cretaceous deposits of the North Sea area in the form of bentonites and as lavas and tuffaceous material (Hallam & Sellwood, 1968; Cowperthwaite *et al.*, 1972; Bradshaw, 1975; Howitt *et al.*, 1975; Knox & Fletcher, 1978; Chowdhury, 1982; Jeans *et al.*, 1982; Hansen & Lindgreen, 1989; Lindgreen, 1991).

GEOLOGICAL SETTING

The most prominent geological feature in East Greenland is the Caledonian mountain belt which stretches from 70°-82°N over a distance of more than 1300 km. It is bordered along its eastern margin by partially uplifted Late Palaeozoic and Mesozoic sedimentary basins (Fig. 1). The Jameson Land basin to the south and the Wollaston Forland basin to the north show marked differences in stratigraphic and structural evolution. The Jameson Land basin contains a relatively complete Upper Palaeozoic sedimentary section more than 10 km thick, topped by a thick Triassic-Lower Cretaceous succession, about 3 km thick. The southern part of the Wollaston Forland basin was transgressed for the first time in Late Permian time. Middle Jurassic-Lower Cretaceous deposits overstep the thin Permian succession towards the north and rests directly on crystalline basement. The Medial to Late Jurassic sedimentary development of the two basins are, however, very similar (Surlyk, 1991).

Devonian-Early Triassic. The Caledonian orogeny culminated in Late Silurian-Early Devonian times and was followed by Devonian extensional collapse of the mountain belt succeeded by Carboniferous rifting. The Devonian succession reaches more than 10 km in thickness and subsidence was governed by extension by strike-slip transtension and rifting. The Upper Permian Foldvik Group rests with pronounced angular unconformity on the eroded and peneplained surface of the older deposits (Surlyk *et al.*, 1986; Surlyk, 1990). The Foldvik Creek Group and the overlying Lower Triassic Wordie Creek Formations form a major transgressive-regressive cycle representing the combined effects of post-Carboniferous thermal subsidence and an important Late Permian rifting event. This tectonically induced cycle is overprinted by the effects of high-amplitude sea-level changes in the latest Permian (Surlyk, unpublished data).

The Foldvik Creek Group consists of a basal terrigenous conglomerate-sandstone-mudstone sheet (Huledal Formation) overlain by a hypersaline carbonate-evaporite unit (Karstryggen Formation) followed by normal marine deposits (Wegener Halvø Formation) and basinal mudstones (Ravnefjeld Formation). In the Jameson Land basin a siliclastic basin fill phase is recognised (Schuchert Dal Formation) reflecting the dramatic end-Permian sea level fall.

The area was, however, rapidly submerged in earliest Triassic time and a marine bay was formed where up to 700 m of grey and green mudstones were deposited (Wordie Creek Formation). By the end of early Triassic, Induan, time, the marine basin was filled, and succeeding Triassic deposition took place in continental environments mainly under dry arid conditions.

Middle Triassic-Lower Cretaceous. The lithostratigraphic nomenclature of the Jurassic succession of East Greenland (Surlyk *et al.*, 1973; Surlyk, 1977) has recently been revised (Surlyk *et al.*, in press) and the new scheme is used here.

In mid-Rhaetian times the depositional basin became areally strongly reduced, to cover only the Jameson Land basin. This restriction lasted through Early Jurassic times and is interpreted as caused by uplift of a major rift dome centered over northern East Greenland (Surlyk, 1978b, submitted; Surlyk *et al.*, 1993). The Rhaetian-Sinemurian Kap Stewart formation is 155-300 m thick, and was deposited in an extensive lake. Black shales were deposited under anoxic conditions in periods of high lake level, whereas deltaic sheet sandstones prograded from the lake margins in periods of marked lake level fall (Dam & Christiansen, 1990; Dam & Surlyk, 1992, 1993).

The first fully marine inundation of the Jameson Land basin since the earliest Triassic took place in Early Jurassic, Pliensbachian time. The Pliensbachian-Aalenian Neill Klinter Group is up to about 500 m thick and was deposited during alternating tidal and poorly oxygenated conditions. It is topped by up to 120 m of black mudstones of the mainly Aalenian Sortehat Formation.

A major change in palaeogeography took place close to the Aalenian-Bajocian transition. The Upper Bajocian-Callovian Vardekløft Group was deposited during a major regional transgression in two tectonically controlled *en echelon* arranged embayments. The formation is 160-600 m thick, and consists of onlapping shallow marine sandstones of the Pelion Formation and laterally equivalent offshore silty mudstones of the Fossilbjerget Formation (Surlyk, 1991; Engkilde, 1994; Engkilde & Surlyk, in press). The onlap probably reflects gradual subsidence of the rift dome, superimposed by a Late Bathonian-Callovian eustatic sea-level rise (Surlyk *et al.*, 1993). Domal uplift was succeeded by rift onset in the Bajocian-Bathonian and rifting reached a climax in Kimmeridgian-Volgian time.

The overall rise in sea-level initiated in the Bathonian culminated in the Late Oxfordian-Kimmeridgian coinciding with increased rifting reflected by widespread deposition of dark-grey mudstones of the Bernbjerg Formation or black shales with thick mass flow sandstones of the Hareelv Formation (Surlyk, 1987, 1991).

Maximum rifting in mid-Volgian times was characterised by deposition of coarse-grained shallow marine syn-rift deposits of the Raukelv Formation (Surlyk, 1978a, 1989; Surlyk & Noe-Nygaard, 1992). The tectonic phase gradually phaded out in the latest Valanginian, and a short-lived relative sea-level fall took place close to the Valanginian-Hauterivian boundary. Succeeding Cretaceous deposition dominated by dark offshore mudstones and coastal sandstones took place under relatively uniform thermal subsidence interrupted by several rift phases in mid Cretaceous time. Post-Valanginian deposits are, however, absent from the Jameson Land basin due to recent erosion and are only known from areas further to the north.

MATERIAL AND METHODS

In the Jameson Land basin, shallow core samples were investigated from the following formations and locations: the Karstryggen, Wegener Halvø, Ravnefjeld, and Hareelv Formations (Figs. 1, 2). Outcrop samples were studied from the Schuchert Dal (Oksedal member) and Wordie Creek Formations, Kap Stewart Group, and Sortehat, Fossilbjerget, Hareelv and Raukelv Formations (Figs. 1, 2). In the Wollaston Forland basin, samples from Barremian, Aptian and Albian mudstones were investigated (Figs. 1, 2).

Only mudstone and shale samples were studied, except for the limestone of the Wegener Halvø Formation. Shallow core samples were from the permafrost layers, whereas outcrop samples were taken immediately above the top of the permafrost.

The samples were hand-ground to pass a 0.2 mm sieve. Before separation in size-fractions, chemical pretreatment involved removal of carbonates (when present) with NaAc at pH 5.5 and 100°C, followed by NaOCl at pH 9.0 and 100°C to remove organic matter (Anderson, 1963), and then Na-dithionite, bicarbonate, and citrate at pH 7 to remove Fe and Al oxides (Mehra & Jackson, 1960), using ~50 mg dithionite per g of sample. The samples were then ultrasonically dispersed. The sand plus silt fraction was removed by centrifugation in a particle-size centrifuge, and the fine clay (<0.2 μm) and coarse clay (0.2-2 μm) fractions were separated in a continuous flow centrifuge. The fine-clay fraction was subdivided into the mixed-layer fraction and a fraction dominated by discrete clay minerals by the ethanol procedure (Hansen & Lindgreen, 1989). The amounts of organic carbon, pyrite and calcite in total samples were determined by DTA-EGA (Morgan, 1977).

For X-ray diffraction (XRD) was used Co*Kα* radiation (β-filter and pulse-height selection) and a Philips PW 1050/80 goniometer with fixed slits. The total sample (<0.2 mm), the sand plus silt, the coarse clay, and the fine clay fractions were analysed by XRD. For XRD of clay fractions, specimens were prepared by the pipette method, using 2.5 mg sample per square centimeter, and for each sample the following specimens were prepared: Mg^{2+}-saturated and air-dry, Mg^{2+}-saturated and glycerolated (for mixed-layer fractions glycolated), and K^{+}-saturated and heated to 300°C. 2.4 x 2.4 cm specimens were analysed with 1/4° divergence and anti-scatter slits in the range 3-25°2θ. The mixed-layer patterns for the Mg^{2+}- saturated and air-dry and the Mg^{2+}- saturated and glycolated specimens were computer-simulated with the NEWMOD program of R.C.Reynolds. It is important to notice that illite and smectite determined by XRD in the studies cited above (Hallam & Sellwood, 1968; Cowperthwaite *et al.*, 1972; Bradshaw, 1975; Howitt *et al.*, 1975; Knox, 1977; Knox & Fletcher, 1978; Chowdhury, 1982; Jeans *et al.*, 1982; Hallam *et al.*, 1991) may actually be I-S with random ordering or segregation of illite and smectite layers (see e.g. Reynolds, 1980). Furthermore, the two-component I-S structures modelled by us may actually be more complicated multi-component mixed-layers having illite and smectite as the main components.

Fine clay fractions (<0.2 μm) of the Schuchert Dal, Wordie Creek, Sortehat and Hareelv Formations were investigated by transmission electron microscopy (TEM) with energy dispersive X-ray elemental analysis (AEM) on a Philips STEM 430 and by Atomic Force Microscopy (AFM) in contact and non-contact mode using a Rasterscope™ 4000.

RESULTS

Preliminary XRD investigations of a large number of mudstone samples show that the clay mineralogy within each formation is relatively uniform, except for the Hareelv Formation (at Sjællandselv, Figs. 1, 2) and for the Lower Cretaceous deposits. Therefore, several samples from these units, and one sample representing each of the other formations and the Hareelv Formation (at Katedralen, Figs. 1, 2) were selected for more detailed study.

Upper Permian-Lower Triassic formations

XRD and DTA-EGA show that the samples beside clay minerals contain quartz (~20%), feldspars, pyrite (~1%, the core samples), and, except the Schuchert Dal Formation, calcite (~2% in the Wordie Creek, 20% in the Ravnefjeld and Karstryggen Formations, and ~70% in the Wegener Halvø Formation).

XRD shows that the coarse clay fractions of the Karstryggen, Wegener Halvø, Ravnefjeld, Schuchert Dal, and Wordie Creek Formations (Fig. 3) contain fair amounts of illite, chlorite (except for the Wegener Halvø Formation which contains large amounts of chlorite), kaolinite, vermiculite, and small amounts of I-S. Resolution of the kaolinite (002) and the chlorite (004) and of the kaolinite (001) and chlorite (002) peaks show that both minerals are present. Kaolinite is, however, absent in the Karstryggen Formation. The fine clay fractions contain chlorite, I-S, and kaolinite in approximately equal amounts (Fig. 4). Upper Permian-Lower Triassic I-S contains ~85% illite layers and is ordered in IS units (Fig. 5).

Rhaetian-Jurassic-Lower Cretaceous formations

AFM shows that relatively large particles are present in the fine-clay fractions of the Sortehat Formation and most of the Hareelv Formation (e.g. Sjællandselv, boring 303115, 17.06 m depth) (Figs. 7 and 8). However, ultra-fine particles dominate in the fine-clay fractions of some mudstones from the Hareelv Formation (Sjællandselv, boring 303116, 26.85 m and 36.98 m depth; Fig. 9)

XRD on randomly oriented specimens shows that the samples contain 10-20% quartz together with feldspars. The core samples contain pyrite (from DTA-EGA up to ~5%), and the outcrop samples traces of jarosite. Significant amounts of clinoptilolite are present in one sample of the Hareelv Formation (Sjællandselv, boring 303115, 13.85 m depth) and fluorapatite is present at two levels of the Hareelv Formation (Sjællandselv, boring 303115, 10.40 m depth; boring 303116, 12.38 and 17.71 m depth). The kaolinite group mineral is a well-crystalline kaolinite in the Kap Stewart Group, and predominantly b-axis disordered kaolinite in the Sortehat, Fossilbjerget and Hareelv Formations. A mica, predominantly

$2M_1$ and trioctahedral, is present in fair amounts in the Fossilbjerget Formation (Katedralen, 555 m) and in the Hareelv Formation (Sjællandselv 303116, 26.85 m and 12.22 m, and 303115, 13.85 m). Optical microscopy of the sand fraction of the samples from Sjællandselv (boring 303116, 26.85 m and 12.22 m depth), confirms the presence of apatite and shows large amounts of biotite.

The Kap Stewart, Sortehat and Fossilbjerget Formations, and most samples from the Hareelv Formation (Fig. 3) have coarse clay fractions dominated by kaolinite and in addition I-S and illite. The fine-clay fractions of the Rhaetian-Sinemurian Kap Stewart Group are dominated by kaolinite, whereas the Aalenian-Kimmeridgian Sortehat, Fossilbjerget and Hareelv Formations contain large amounts of kaolinite and I-S (Fig. 4).

Three samples from the Hareelv Formation, however, have coarse clay fractions dominated by I-S with a large amount of smectite layers and in addition kaolinite and traces of illite (Sjællandselv, boring 303116, 13.24 m, 36.30 m, and 36.98 m depth, the last two samples in the same mudstone unit) (Fig. 10). The fine-clay fractions are similarly dominated by I-S with a large amount of smectite layers (Fig. 11).

A third clay mineralogy is seen in another sample from the Hareelv Formation (Sjællandselv, boring 303116, 26.85 m depth). The coarse clay fraction contains large amounts of mixed-layer illite-vermiculite (I-V) and kaolinite, and fair amounts of vermiculite and illite (Fig. 10). The fine-clay fractions similarly contains large amounts of I-V and, in addition, some vermiculite (Fig. 11).

A similar clay mineralogy is seen in the samples from Lower Volgian mudstones (Salix Dal Member). An exception is sample 255182 which in the fine-clay fraction contains I-S with a large amount of smectite layers together with illite and kaolinite.

Two of the three Barremian shales (342092 and 342231) from Kuhn Ø and Wollaston Forland, one (351573) of the three Aptian and one (351587) of the two Albian shales from Wollaston Forland resemble the Sortehat and Fossilbjerget mudstones. They have coarse clay fractions with large amounts of kaolinite, together with some illite, smectite and I-S, whereas the fine-clay fractions contain large amounts of kaolinite and I-S. The third Barremian sample (342236) from Wollaston Forland is similar to the first two, except for a larger content of smectite layers in both coarse and fine-clay fractions.

The two other Aptian mudstones (342170 and 342167) from Wollaston Forland have a coarse clay fraction with large amounts of smectite layers and small amounts of kaolinite and illite. The fine-clay fraction is dominated by I-S having a high proportion of smectite layers and contains in addition small amounts of kaolinite.

The other Albian mudstone (342194) from Wollaston Forland has a coarse clay fraction with large amounts of kaolinite and smaller amounts of illite, smectite and I-S. The fine-clay fraction contains large amounts of kaolinite and smectite and of I-S.

I-S from the Sortehat and Fossilbjerget Formations and from the Hareelv Formation at Katedralen contains 85% illite layers and are semi-ordered in IS units. I-S from some samples of the Hareelv Formation at Sjællandselv (e.g. boring 303115, 17.06 m depth) contain app. 80% illite layers and have segregation of illite and smectite layers. In contrast, I-S from some samples of the Hareelv Formation at Sjællandselv (e.g. boring 303116, 36.98 m depth) have 30% illite layers and random ordering. In some Barremian samples (e.g. 342092) the I-S contain app. 80% illite layers and are ordered in IS units. In the Aptian sample 342170 the I-S contains 50% illite layers and is randomly ordered, and in the Albian sample 342194 the I-S has 80% illite layers and has a tendency to ordering in IS units (Fig. 6).

DISCUSSION

Post-depositional changes in clay mineralogy

Weathering. The sedimentary rocks of Jameson Land have been eroded and weathered following major Tertiary uplift. However, significant amounts of pyrite and, in Upper Permian-Lower Triassic samples, of chlorite are present, and the clay mineralogy of outcrop and core samples is the same for each formation. This indicates that post-depositional weathering of clay minerals is insignificant despite the presence of jarosite in several samples.

Diagenesis. In the investigated Upper Permian-Jurassic mudstones, the presence of I-S with max. 70%-90% illite layers, kaolinite and sometimes vermiculite, shows that at most the middle-diagenetic stage of maturity has been reached

(Frey, 1970; Foscolos *et al.*, 1976). The change in I-S, from ~85% illite and IS-ordering in the Upper Permian-Lower Triassic to ~80% illite and semi-ordering in the Aalenian-Oxfordian mudstones could result from diagenesis at the temperature of oil generation or from different weathering conditions and source materials. The Upper Permian-Lower Triassic rocks investigated are immature for oil generation (Surlyk *et al.*, 1986). The change in clay mineralogy accompanied by a disappearance of chlorite and a significant increase in the amount of kaolinite supports the hypothesis of different weathering conditions in the provenance areas, since chlorite and kaolinite are stable in different weathering regimes (see below).

In sandstones, the chemistry of percolating waters controls the clay mineralogical processes (Millot, 1970; Hoffman & Hower, 1979). The Kap Stewart Group is dominated by interbedded dark shales and arkosic sandstones with a few thin coal seams. Percolating, weakly acid meteoric waters may have formed the kaolinite in the same way as has been suggested for similar deposits in the Brent Group of the North Sea (Hancock & Taylor, 1978) and in the Cambrian sandstones of Sahara (Millot, 1970). The fact that the kaolinite mineral in the Kap Stewart Formation is well-crystalline support this assumption, since most kaolinites in unconsolidated sediments are disordered and only become ordered during diagenesis (Shutov *et al.*, 1970; Hoffman & Hower, 1979). The high proportion of kaolinite in the mudstones of the Kap Stewart Group compared to the other formations is thus predominantly due to a diagenetic process.

The influence of diagenesis on the discrete clay minerals is thus considered to be insignificant except for the shales of the Kap Stewart Group, and these minerals are predominantly derived from erosion in the source areas and subsequently transported into the basin.

Origin of detrital clay minerals

Volcanic clays. The Rhaetian-Jurassic shales are generally dominated by kaolinite with subordinate illite and I-S having 25% smectite and semi-ordering. A similar clay mineralogy is found in the Hareelv Formation (Sjællandselv, boring 303115, 17.06 m and 29.71 m) (Figs. 3, 4, 6, 10, 11). These clays are probably the result of weathering in a subtropical climate (see below). However, two mudstone units in the Hareelv Formation (Sjællandselv, boring 303116, 13.24 m and 36.30-36.98 m depth) are totally different. They are dominated by I-S with a high content of smectite (~70%) and random ordering. This clay mineralogy and the presence of large amounts of biotite and fluorapatite indicate a volcanic origin (Grim & Güven, 1978). These two units are thus probably volcanic clays, reflecting episodes of volcanic activity in the Kimmeridgian. Mudstone units having I-S with 40% smectite and random ordering (Sjællandselv, boring 303116, 12.38 m and 17.71 m depth) may also contain volcanic material. Small-scale variation between abundant and little smectite in adjacent beds in the Bathonian of eastern England (Bradshaw, 1975) and in the Corallian of southern England (Chowdhury, 1982) was similarly explained as representing periodic volcanism. The English bentonites with abundant smectite also contain biotite and apatite like the East Greenland examples, and possibly christobalite which also may be present in our samples, since we similarly observe a 4.06 Å XRD peak. The British Corallian bentonite beds in addition contained a zeolite of the clinoptilolite-heulandite series, similarly to the significant amounts of clinoptilolite in one sample from the Hareelv Formation (Sjællandselv, boring 303115, 13.85 m depth). Deposition of sand bodies of mass flow origin in the Hareelv Formation was attributed to the triggering effect of earthquakes associated with rifting (Surlyk, 1987). The large amounts of smectite in the Aptian clays from Wollaston Forland are probably also of volcanic origin.

The probably volcanic smectites in the Kimmeridgian part of the Hareelv Formation of East Greenland are only slightly older than those in the Middle-Upper Volgian Farsund and Mandal Formations in wells 2/7-3 and W1 in the Central Trough of the central North Sea (Hansen & Lindgreen, 1989; Lindgreen, 1991). Similarly, the probably volcanic smectites in the Aptian mudstones from Wollaston Forland are similar to the Upper Aptian-Lower Albian volcanic bentonites of southern England (Jeans *et al.*, 1982). This indicates roughly contemporaneous volcanism in the two regions and conforms with the well-known similarity in tectonic-stratigraphic evolution of the rift basins of East Greenland and the North Sea which are part of a major rift complex in the North European-North Atlantic region (Surlyk 1978b, 1990, submitted).

Palaeoclimatic influence. The main sediment source during Late Permian-Early Cretaceous time was weathered Precambrian and Caledonian crystalline rocks. The clay mineralogy in the Upper Permian and Lower Triassic mudstones (illite, chlorite, vermiculite, small amounts of kaolinite, and I-S having ~85% illite and IS-ordering) is typical for a semi-arid climate and similar to the clay mineralogy in the Devonian and Lower Carboniferous of Scotland (Wilson, 1971). The source material for the Upper Permian-Lower Triassic mudstones possibly also included weathered Devonian redbeds. The Carboniferous succession was, however, deposited in a more humid climate which by analogy with the Scottish conditions may be dominated by kaolinite formed by weathering in a wet tropical climate (Wilson *et al.*, 1972). In contrast, the Jurassic mudstones of Jameson Land contain large amounts of kaolinite, I-S having ~80 % illite and semi-ordering, and illite, but no chlorite. This change could be due to increased leaching in Jurassic time, probably due to increased precipitation (Millot, 1970). Investigations of the relationship between climate and clay mineralogy (Barshad, 1966; van der Merwe & Weber, 1963) suggest that the large amounts of kaolinite and significant amounts of illite and smectite layers in the Jurassic mudstones of East Greenland reflect a subtropical climate with a rainfall of 500-800 mm. Consequently, the hypothesis that the large kaolinite content in Jurassic mudstones results from uplift and erosion of kaolinitic regoliths formed during Carboniferous time in a humid, tropical climate (Hurst, 1985b) is not necessary to explain the large kaolinite content in the Jurassic mudstones of East

Greenland.

The nature of the detrital material seems to be the same through the Upper Bajocian-Middle Callovian Fossilbjerget Formation and the Upper Oxfordian-Kimmeridgian Hareelv Formation. One exception is, however, the occurrence of bentonitic I-S with a high proportion of smectite layers in the Kimmeridgian part of the Hareelv Formation of the Jameson Land basin and in the Aptian of the Wollaston Forland basin. Another exception is the vermiculitic clays in one sample from the Hareelv Formation (Sjællandselv, boring 303116, 26.88m depth) and in the Lower Volgian Salix Dal Member mudstones at Sjællandselv. These vermiculitic mudstones most likely formed from weathering of micas, derived from erosion of elevated fault block crests and rift shoulders to the north (Surlyk, 1991). This change in sediment source explains the occurrence of IS ordered I-S with 80% illite layers in the Barremian mudstones. This type of I-S is normally formed during diagenesis simultaneously with oil generation at temperatures of app. 100°. Its occurrence in the Barremian mudstones having undergone only low temperature transformation demonstrates the importance of source area effects in diagenetis studies. Similar source-derived IS-ordered I-S was found by Hurst (1982) in Devonian sediments from Scotland.

Hallam *et al.* (1991) suggested a climatic change towards a more arid climate in Late Jurassic time mainly on the basis of a decrease in kaolinite in the European clays. The fluctuations in the amount of smectite layers during the Late Jurassic-Early Cretaceous in East Greenland are probably due to periodic volcanism as suggested for similar occurrences in sourthern England and northern Ireland by Cowperthwaite *et al.* (1972) and Jeans *et al.* (1982). The high-smectitic bands are similar in mineralogy to the bentonite bands of the Jurassic and Cretaceous of Northwest Europe (Hallam *et al.*, 1991). Apart from these bands, the samples investigated by us contain large amounts of kaolinite. As an alternative to the climate-control mechanism, the decrease in amount of kaolinite towards the end of the Jurassic in samples discussed by Hallam *et al.* (1991) might reflect larger distances to the source areas (cf. Chamley *et al.*, 1983; Deconinck *et al.*, 1985). This alternative is also mentioned by Wignall & Ruffell (1990) and Hallam *et al.* (1991). The absence of a large-scale shift to less kaolinite in the Upper Jurassic-Lower Cretaceous of East Greenland having a well-defined and constant source area suggests that the change to less kaolinite in England and France (Hallam *et al.*, 1991) may be due to larger distances to source areas probably during a major Late Jurassic rise in sea level. Wignall & Ruffell (1990, p. 370) actually states that "the aridity increase occurs at a time of high sea level stand during continental break up".

ACKNOWLEDGEMENTS

We are grateful to S.Piasecki and H.Nøhr-Hansen of the Geological Survey of Denmark and Greenland for supplying some of the samples and for providing stratigraphic information. We thank A. Henschel, Institute of Physics, Technical University of Denmark, for carrying out the STEM investigations. The project was supported by the Ministry of Energy (EFP grant), the Carlsberg Foundation and the Danish Natural Science Research Foundation.

REFERENCES

Ahn J.H. & Peacor D.R. (1985) Transmission electron microscopic study of diagenetic chlorite in Gulf Coast argillaceous sediments. *Clays Clay Miner.* 33, 228-236.

Ahn J.H. & Peacor D.R. (1987) Transmission electron microscopic study of the diagenesis of kaolinite in Gulf Coast argillaceous sediments. Pp. 151-157 in: *Proc. Int. Clay Conf., 1985, Denver,* (L. G. Schultz, H. van Olphen & F. A. Mumpton, editors), Clay Miner. Soc., Bloomington, Indiana.

Anderson J.U. (1963) An improved pretreatment for mineralogical analysis of samples containing organic matter. *Clays Clay Miner.* 10, 380-388.

Barshad I. (1966) The effect of variation in precipitation on the nature of clay mineral formation in soils from acid and basic igneous rocks. Pp. 167-173 in: *Proc. Int. Clay Conf., 1966, Jerusalem*, (L. Heller & A. Weiss, editors). Israel Prog. Sci. Translations, Jerusalem, 1.

Bradshaw M.J. (1975) Origin of montmorillonite bands in the Middle Jurassic of eastern England. *Earth Planet. Sci. Lett.* 26, 245-252.

Chamley H., Debrabant P., Candillier A.-M. & Foulon J. (1983) Clay mineralogy and inorganic geochemical stratigraphy of Blake-Bahama Basin since the Callovian, site 534, Deep Sea Drilling Project leg 76. *Init. Rep. DSDP* 76, 437-451.

Chowdhury A.N. (1982) Smectite, zeolite, biotite and apatite in the Corallian (Oxfordian) sediments of the Baulking area in Berkshire, England. *Geol. Mag.* 119, 487-496.

Cowperthwaite I.A., Fitch F.J., Miller J.A., Mitchell J.G. & Robertson R.M.S. (1972) Sedimentation, petrogenesis and radioisotopic age of the Cretaceous Fuller's Earth of Southern England. *Clay Miner.* **9**, 309-327.

Dam G. & Christiansen F.G. (1990) Organic geochemistry and source potential of the lacustrine shales of the Late Triassic-Early Jurassic Kap Stewart Formation: *Marine Pet. Geol.* **7**, 428-443.

Dam G. & Surlyk F. (1992) Forced regressions in a large wave- and storm-dominated anoxic lake, Rhaetian-Sinemurian Kap Stewart Formation, East Greenland. *Geology* **20**, 749-752.

Dam G. & Surlyk F. (1993) Cyclic sedimentation in a large wawe and storm-dominated anoxic lake, Kap Stewart Formation (Rhaetian-Sinemurian), Jameson Land, East Greenland. Pp. 419-448 in: *Sequence Stratigraphy and Facies Associations*, (H. W. Posamentier, D. P. Summerhayes, B. U. Haq & G. P. Allen, editors). *Spec. Publs. Int. Ass. Sediment.* **18**.

Deconinck J.-F., Beaudoin B., Chamley H., Joseph P. & Raoult J.F. (1985) Contrôles techtonique, eustatique et climatique de la sédimentation argileuse du domaine subalpin français au Malm-Crétacé. *Rev. Géol. Dyn. Géogr. Phys.* **26**, 311-320.

Engkilde M. (1994) The Middle Jurassic Vardekløft Formation, East Greenland: depositional environments and sequence stratigraphy of shallow marine sandstones deposited in a low-gradient epeiric seaway. Ph.D. Thesis, Univ. Copenhagen, 207 pp.

Engkilde M. & Surlyk F. (submitted) Sequence stratigraphy of the Middle Jurassic shallow marine Vardekløft Group, East Greenland. In: *The Jurassic of Denmark and Greenland*. (J. R. Ineson & F. Surlyk, editors). The Geological Survey of Denmark and Greenland.

Foscolos A.E., Powell T.G. & Gunther P.R. (1976) The use of clay minerals and inorganic and organic geochemical indicators for evaluating the degree of diagenesis and oil generating potential of shales. *Geochim. Cosmochim. Acta* **40**, 953-966.

Frey M. (1970) The step from diagenesis to metamorphism in pelitic rocks during Alpine orogenesis. *Sedimentology* **15**, 261-279.

Grim R.E. & Güven N. (1978) *Bentonites. Geology, Mineralogy, Properties and Uses. Dev. Sedimentology* **24**, Elsevier, Amsterdam, 256 pp.

Hallam A., Grose J.A. & Ruffell A.H. (1991) Palaeoclimatic significance of changes in clay mineralogy across the Jurassic-Cretaceous boundary in England and France. *Palaeogeogr., Palaeoclimatol., Palaeoecol.* **81**, 173-187.

Hallam A. & Sellwood B.W. (1968) Origin of Fuller's Earth in the Mesozoic of Southern England. *Nature* **220**, 1193-1195.

Hancock N.J. & Taylor A.M. (1978) Clay mineral diagenesis and oil migration in the Middle Jurassic Brent Sand Formation. *J. Geol. Soc. London* **135**, 69-72.

Hansen P.L. & Lindgreen H. (1989) Mixed-layer illite/smectite diagenesis in Upper Jurassic claystones from the North Sea and onshore Denmark. *Clay Miner.* **24**, 197-213.

Hoffman J. & Hower J. (1979) Clay mineral assemblages as low grade metamorphic geothermometers: application to the thrust faulted Disturbed Belt of Montana, U.S.A. *Soc. Econ. Paleont. Mineral., Sp. pap.* 26, 55-79.

Hower J., Eslinger E.V., Hower M.E. & Perry E.A. (1976) Mechanism of burial metamorphism of argillaceous sediment: 1. Mineralogical and chemical evidence. *Bull. Geol. Soc. Amer.* 87, 725-737.

Howitt F., Aston E.R. & Jaqué M. (1975) The occurrence of Jurassic volcanics in the North Sea. Pp. 379-387 in: *Petroleum and the Continental shelf of North-West Europe* 1, (A. W. Woodland, editor). Appl. Sci. Publ., London.

Hurst A. (1982) The clay mineralogy of Jurassic shales from Brora, NE Scotland. Pp. 677-684 in: *Proc. Int. Clay Conf. Bologna and Pavia, Italy, 1981* (H. van Olphen & F. Veniale, editors). Elsevier, Amsterdam.

Hurst A. (1985a) Diagenetic chlorite formation in some Mesozoic shales from the Sleipner area of the North Sea. *Clay Miner.* 20, 69-80.

Hurst A. (1985b) The implications of clay mineralogy to palaeoclimate and provenance during the Jurassic in NE Scotland. *Scott. J. Geol.* 21, 143-160.

Jeans C.V., Merriman R.J., Mitchell J.G. & Bland D.J. (1982) Volcanic clays in the Cretaceous of Southern England and Northern Ireland. *Clay Miner.* 17, 105-156.

Knox R.W.O'B. (1977) Upper Jurassic pyroclastic rocks in Skye, west Scotland. *Nature* 265, 323-324.

Knox R. W. O'B. & Fletcher B.N. (1978) Bentonites in the lower D beds (Ryazanian) of the Speeton Clay of Yorkshire. *Proc. Yorkshire Geol. Soc.* **42**, 1937-1943.

Lindgreen H. (1991) Elemental and structural changes in illite/smectite mixed-layer minerals during diagenesis in Kimmeridgian-Volgian (-Ryazanian) clays in the Central Trough, North Sea and the Norwegian-Danish Basin. Bull. *Geol. Soc. Denmark* **39**, 1-82.

Mehra O. & Jackson M.L. (1960) Iron oxide removal from soils and clays by a dithionite-citrate system buffered with sodium bicarbonate. *Clays Clay Miner.* **7**, 317-327.

van der Merwe C.R. & Weber H.W. (1963) The clay minerals of South African soils developed from granite under different climatic conditions. *S. Afr. J. Agric. Sci.* **6**, 411-454.

Millot G. (1970) *Geology of clays.* Springer Verlag, London, 429pp.

Milne I.H. & Earley J.W. (1958) Effect of source and environment on clay minerals. *Amer. Ass. Pet. Geol. Bull.* **42**, 328-338.

Morgan D.J. (1977) Simultaneous DTA-EGA of minerals and natural mineral mixtures. *J. Thermal Analysis* **12**, 245-263.

Pearson M.J. & Small J.S. (1988) Illite-smectite diagenesis and paleotemperatures in northern North Sea Quarternary to Mesozoic shale sequences. *Clay Miner.* **23**, 109-132.

Reynolds R.C. (1980) Interstratified clay minerals. Pp. 249-404 in: *Crystal Structures of Clay Minerals and their X-ray Identification.* (G. W. Brindley & G. Brown, editors). Mineral. Soc., London.

Shutov V.D., Aleksandrova A.V. & Losievskaya S.A. (1970) Genetic interpretation of the polymorphism of the kaolinite group in sedimentary rocks. *Sedimentology* 15, 69-72.

Surlyk F. (1977) Stratigraphy, techtonics and palaeogeography of the Jurassic sediments of the areas north of Kong Oscars Fjord, East Greenland. *Bull. Grønlands Geol. Unders.* 123, 1-56.

Surlyk F. (1978a) Submarine fan sedimentation along fault scarps on tilted fault blocks (Jurassic Cretaceous boundary, East Greenland). *Bull. Grønlands Geologiske Undersøgelse* 128, 1-108.

Surlyk F. (1978b) Jurassic basin evolution of East Greenland. *Nature* 274, 130-133.

Surlyk F. (1987) Slope and deep shelf gully sandstones, Upper Jurassic, East Greenland. *Amer. Ass. Pet. Geol. Bull.* *71*, 464-475.

Surlyk F. (1989) Mid-Mesozoic syn-rift turbidite systems: controls and predictions. Pp. 231-241 in: *Correlation in Hydrocarbon Exploration,* (J. D. Collinson, editor). Norwegian Pet. Soc., Graham and Trotman, London.

Surlyk F. (1990) Timing style and sedimentary evolution of Late Paleozoic-Mesozoic extensional basins of East Greenland. Pp. 107-125 in: *Tectonic Events Responsible for Britain's Oil and Gas Reserves,* (R. F. P. Hardman & J. Brooks, editors). *Geol. Soc. Spec. Publ.* 55.

Surlyk F. (1991) Sequence stratigraphy of the Jurassic-Lowermost Cretaceous of East Greenland. *Amer. Ass. Pet.*

Geol. Bull. **75**, 1468-1488.

Surlyk F. (submitted) Jurassic domes in the North Sea-northern North Atlantic region. *J. Geol. Soc.*

Surlyk F., Callomon J.H., Bromley R.G. & Birkelund T. (1973) Stratigraphy of the Jurassic-Lower Cretaceous Sediments of Jameson Land and Scoresby Land, East Greenland. *Meddr. Grønland* **193/5**, 1-104.

Surlyk F., Dam G., Engkilde M., Hansen C.F., Kobbelhus E.B., Larsen M., Noe-Nygaard N., Piasecki S. & Vosgerau H. (in press) A new lithostratigraphic scheme for the Jurassic of East Greenland.

Surlyk F., Hurst J.M., Piasecki S., Rolle F., Scholle P.A., Stemmerik L. & Thomsen E. (1986) The Permian of the western margin of the Greenland Sea- A future exploration target. Pp. 629-659 in: *Future Petroleum Provinces of the World,* (M. T. Halbouty, editor). *AAPG Memoir* **40**.

Surlyk F. & Noe-Nygaard N. (1992) Sand bank and dune facies architecture of a wide intracratonic seaway: Late Jurassic-Early Cretaceous Raukelv Formation, Jameson Land, East Greenland. Pp. 261-276 in: *The Three Dimensional Facies Architecture of Terrigenous Clastic Sediments and its Implications for Hydrocarbon Discovery and Recovery* (A. D. Miall & N. Tyler, editors). *SEPM (Society for Sedimentary Geology), Concepts and Model Series 3*.

Surlyk F., Noe-Nygaard N. & Dam G. (1992) High and low resolution sequence stratigraphy in lithological prediction- examples from the Mesozoic around the northern North Atlantic. Pp. 199-214 in: *Petroleum Geology of Northwest Europe: Proceedings of the 4th Conference* (J. R. Parker, editor). The Geological Society of London.

Weaver C.E. (1959) The clay petrology of sediments. *Clays Clay Miner.* **14**, 154-187.

Weaver C.E. & Beck K.C. (1971) Clay water diagenesis during burial: how mud becomes gneiss. *Geol. Soc. Amer. Spec. Pap.* **134**, 1-78.

Wignall P.B. & Ruffell A.H. (1990) The influence of a sudden climatic change on marine deposition in the Kimmeridgian of North West Europe. *J. Geol. Soc. London* **147**, 365-372.

Wilson M.J. (1971) Clay mineralogy of the Old Red Sandstone (Devonian) of Scotland. *J. Sed. Petrol.* **41**, 995-1007.

Wilson M.J., Bain D.C., McHardy W.J. & Barrow M.L. (1972) Clay-mineral studies on some carboniferous sediments in Scotland. *Sediment. Geol.* **8**, 137-150.

FIGURE CAPTIONS

Fig. 1. Geological sketch map showing sample localities. 1: Triaselv (Lowermost Triassic, Scythian, Wordie Creek Formation). 2: Triaselv (Uppermost Permian, Schuchert Dal Formation, Oksedal Member). 3: Triaselv north (Upper Permian, Karstryggen Formation). 4: Triaselv south (Upper Permian, Wegener Halvø and Ravnefjeld Formations). 5: Katedralen (Bajocian-Callovian Fossilbjerget Formation, and Upper Oxfordian-Kimmeridgian Hareelv Formation). 6: Sortehat (Aalenian Sortehat Formation). 7: Sjællandselv (Upper Oxfordian-Lower Volgian Hareelv Formation). 8: Ranunkeldal (Rhaetian-Sinemurian Kap Stewart Formation).

Fig. 2. Stratigraphic scheme of the Upper Permian-Lower Cretaceous of Jameson Land and Wollaston Forland Basins, East Greenland. Mudstone units investigated for clay mineralogy indicated with *. Tectonic phases and occurrence of volcanic clays are shown to the right.

Fig. 3. XRD traces of Mg^{2+}-saturated and air-dried oriented specimens of 2-0.2 μm fractions of Upper Permian-Upper Jurassic mudstones of Jameson Land and Lower Cretaceous mudstones from Kuhn Ø and Wollaston Forland. The Hareelv Formation sample is from the outcrop at Katedralen (5 in fig. 1). Co*Kα*-radiation. Sample localities and stratigraphic position of mudstone samples are shown in Figs. 1, 2. Note that only age is given for the three Lower Cretaceous samples as this part of the succession has not been lithostratigraphically subdivided.

Fig. 4. XRD traces of Mg^{2+}-saturated and air-dried oriented specimens of <0.2 μm fractions of Upper Permian-Upper Jurassic mudstones from Jameson Land and Lower Cretaceous mudstones from Kuhn Ø and Wollaston Forland. The sample of the Hareelv Formation is from the outcrop at Katedralen (5 in Fig. 1). Co*Kα*-radiation. Stratigraphic position of mudstone samples shown in Fig. 2.

Fig. 5. XRD traces of Mg^{2+}- saturated and glycolated oriented specimens of mixed-layer fractions of Upper Permian-Upper Jurassic mudstones from Jameson Land. A: Hareelv Formation (Sjællandselv boring 303116, 36.98 m); B: Sortehat Formation; C: Wordie Creek Formation; D: Schuchert Dal Formation; E: Ravnefjeld Formation. Co*Kα*-radiation. Stratigraphic position of mudstone samples shown in Fig. 2.

Fig. 6. XRD traces of Mg^{2+}- saturated and glycolated oriented specimens of mixed-layer fractions of an Upper Jurassic mudstone from Jameson Land and Lower Cretaceous mudstones from Kuhn Ø and Wollaston Forland. A: Albian; B: Aptian; c: Barremian; D: Hareelv formation (Sjællandselv boring 303115, 17.06 m). Co*Kα*-radiation. Stratigraphic position of mudstone samples shown in Fig. 2.

Fig.7. Atomic force micrographs of the <0.2 μm fraction of a sample from the Kap Stewart Group. Contact mode, pyramidal tip. Scale in the z-direction is from black to white 750 Å. Image is 20,000 by 20000 Å. Plot along the black line is

shown to the right. Vertical distance between marks is 95 Å.

Fig. 8. Atomic force micrographs of the <0.2 μm fraction of a sample from the Hareelv Formation (Sjællandselv, boring 303115, 17.06 m depth). Non-contact mode. Scale in the z-direction is from black to white 1200 Å. Image is 10,000 by 10,000 Å. Plot along the black line is shown to the right. Vertical distance between marks is 105 Å.

Fig. 9. Atomic force micrographs of the <0.2 μm fraction of a sample from the Hareelv Formation (Sjællandselv, boring 303116, 36.98 m depth). Non-contact mode. Scale in the z-direction is from black to white 210 Å. Image is 10,000 by 10,000 Å. Plot along the black line is shown to the right. Vertical distance between marks is 38 Å.

Fig. 10. XRD traces of Mg^{2+}- saturated and air-dried oriented samples of 2-0.2 μm fractions of Upper Jurassic Hareelv Formation mudstones (Sjællandselv, Jameson Land, borings 303115 and 303116. Depths are in m below surface; 7 in Fig. 1). Co*Kα*-radiation. Stratigraphic position of mudstones shown in Fig. 2.

Fig. 11. XRD traces of Mg^{2+}- saturated and air-dried oriented samples of <0.2 μm fractions of Upper Jurassic Hareelv Formation mudstones (Sjællandselv, Jameson Land, borings 303115 and 303116. Depths are in m below surface; 7 in Fig. 1). Co*Kα*-radiation. Stratigraphic position of mudstones shown in Fig. 2.

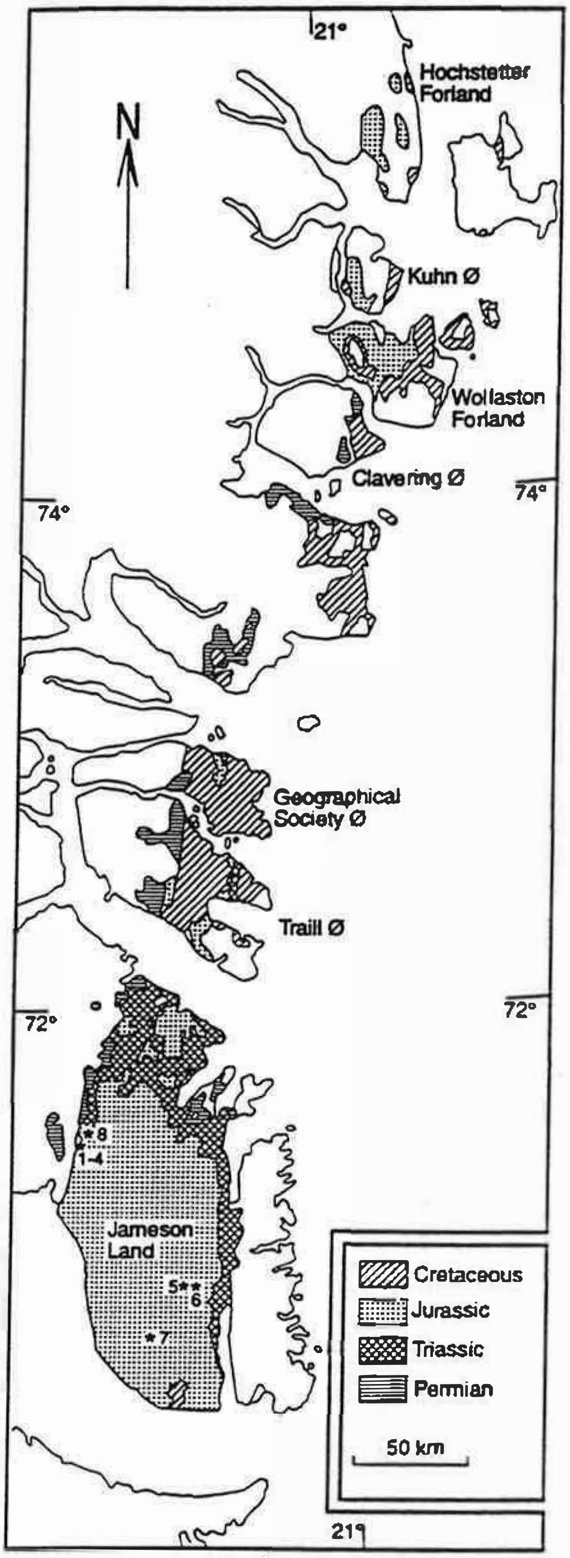
21°
Hochstetter Forland
N
Kuhn Ø
Wollaston Forland
Clavering Ø
74°
74°
Geographical Society Ø
Traill Ø
72°
72°
8
1-4
Jameson Land
5
6
7
Cretaceous
Jurassic
Triassic
Permian
50 km
21°

Fig. 1

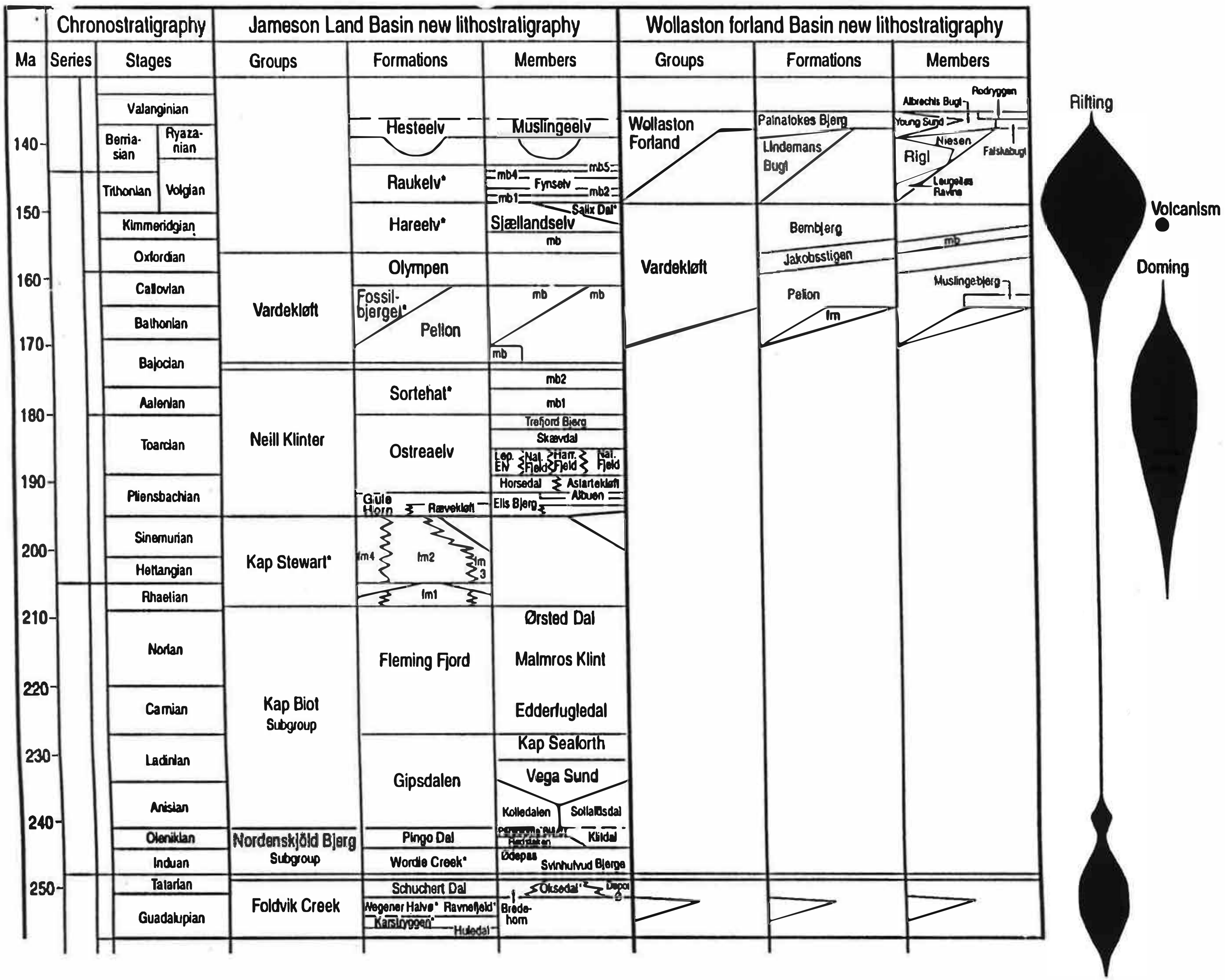
Chronostratigraphy
Jameson Land Basin new lithostratigraphy
Wollaston forland Basin new lithostratigraphy
Ma
Series
Stages
Groups
Formations
Members
Groups
Formations
Members
140
150
160
170
180
190
200
210
220
230
240
250
Valanginian
Berria-sian
Ryaza-nian
Trithonian
Volgian
Kimmeridgian
Oxfordian
Callovian
Bathonian
Bajocian
Aalenian
Toarcian
Pliensbachian
Sinemurian
Hettangian
Rhaetian
Norian
Carnian
Ladinian
Anisian
Olenikian
Induan
Tatarian
Guadalupian
Vardekløft
Neill Klinter
Kap Stewart*
Kap Biot
Subgroup
Nordenskjöld Bjerg
Subgroup
Foldvik Creek
Hesteelv
Raukelv*
Hareelv*
Olympen
Fossil-bjergel*
Pelion
Sortehat*
Ostreaelv
Gule Horn
Rævekløft
fm4
fm2
fm3
fm1
Fleming Fjord
Gipsdalen
Pingo Dal
Wordie Creek*
Schuchert Dal
Wegener Halvø*
Ravnefjeld*
Karstryggen*
Huledal
Muslingeelv
mb4
mb5
Fynselv
mb1
mb2
Salix Dal*
Sjællandselv
mb
mb
mb
mb
mb2
mb1
Trefjord Bjerg
Skævdal
Lep. EN
Nat. Fjeld
Harr. Fjeld
Nat. Fjeld
Horsedal
Astartekløft
Albuen
Elis Bjerg
Ørsted Dal
Malmros Klint
Edderfugledal
Kap Seaforth
Vega Sund
Kolledalen
Sollakisdal
Klitdal
Ødepas
Svinhufvud Bjerge
Oksedal*
Depot
Brede-hom
Wollaston Forland
Vardekløft
Palnatokes Bjerg
Lindemans Bugt
Bernbjerg
Jakobsstigen
Pelion
fm
Albrechts Bugt
Rødryggen
Young Sund
Niesen
Rigl
Falskebugt
Laugeites Ravine
mb
Muslingebjerg
Rifting
Volcanism
Doming

Fig. 2

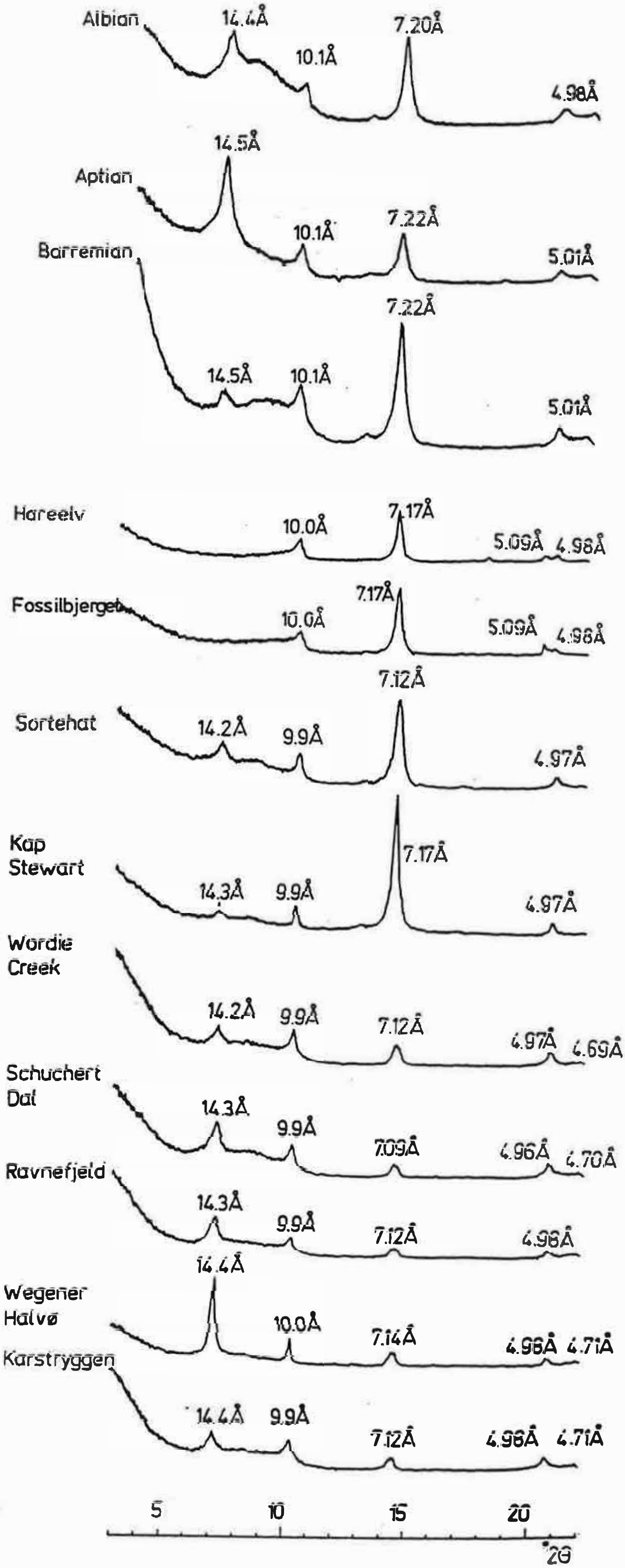
Albian
14.4Å
10.1Å
7.20Å
4.98Å
Aptian
14.5Å
10.1Å
7.22Å
5.01Å
Barremian
7.22Å
14.5Å
10.1Å
5.01Å
Hareelv
10.0Å
7.17Å
5.09Å
4.98Å
Fossilbjerget
7.17Å
10.0Å
5.09Å
4.98Å
Sortehat
7.12Å
14.2Å
9.9Å
4.97Å
Kap Stewart
7.17Å
14.3Å
9.9Å
4.97Å
Wordie Creek
14.2Å
9.9Å
7.12Å
4.97Å
4.69Å
Schuchert Dal
14.3Å
9.9Å
7.09Å
4.96Å
4.70Å
Ravnefjeld
14.3Å
9.9Å
7.12Å
4.98Å
Wegener Halvø
14.4Å
10.0Å
7.14Å
4.98Å
4.71Å
Karstryggen
14.4Å
9.9Å
7.12Å
4.98Å
4.71Å
5
10
15
20
°2θ

Fig. 3

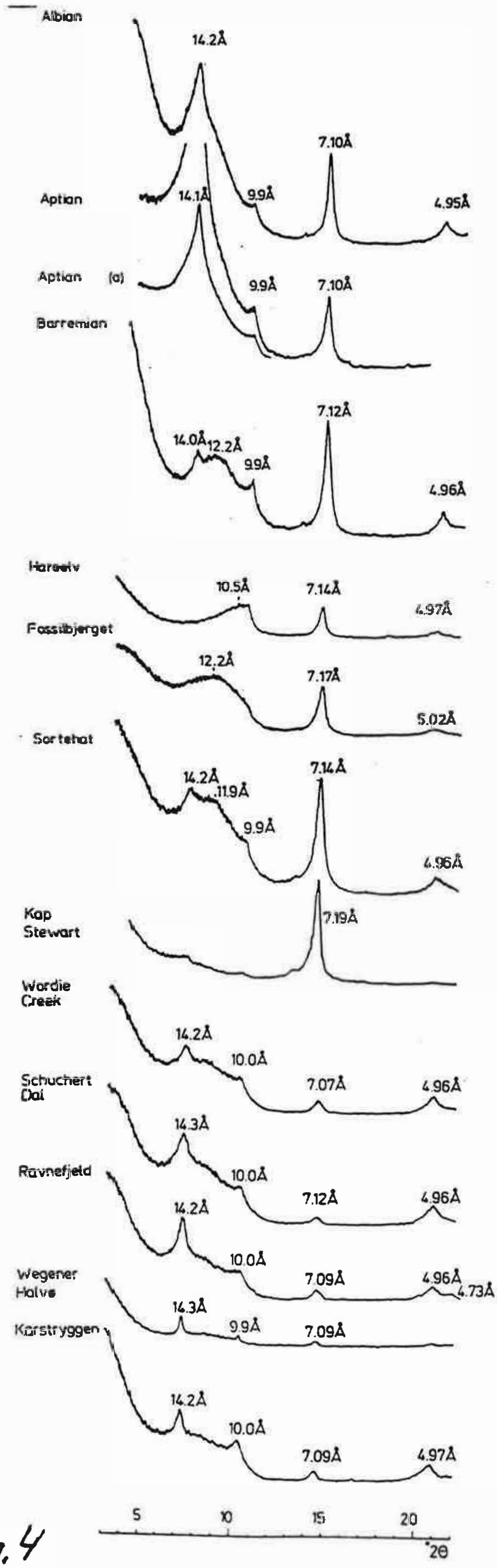

Albian
14.2Å
7.10Å
Aptian
14.1Å
9.9Å
4.95Å
Aptian (a)
9.9Å
7.10Å
Barremian
7.12Å
14.0Å
12.2Å
9.9Å
4.96Å
Hareelv
10.5Å
7.14Å
4.97Å
Fossilbjerget
12.2Å
7.17Å
5.02Å
Sortehat
14.2Å
7.14Å
11.9Å
9.9Å
4.96Å
Kap Stewart
7.19Å
Wordie Creek
14.2Å
10.0Å
7.07Å
4.96Å
Schuchert Dal
14.3Å
10.0Å
7.12Å
4.96Å
Ravnefjeld
14.2Å
10.0Å
7.09Å
4.96Å
4.73Å
Wegener Halvø
14.3Å
9.9Å
7.09Å
Karstryggen
14.2Å
10.0Å
7.09Å
4.97Å
5
10
15
20
°2θ

Fig. 4

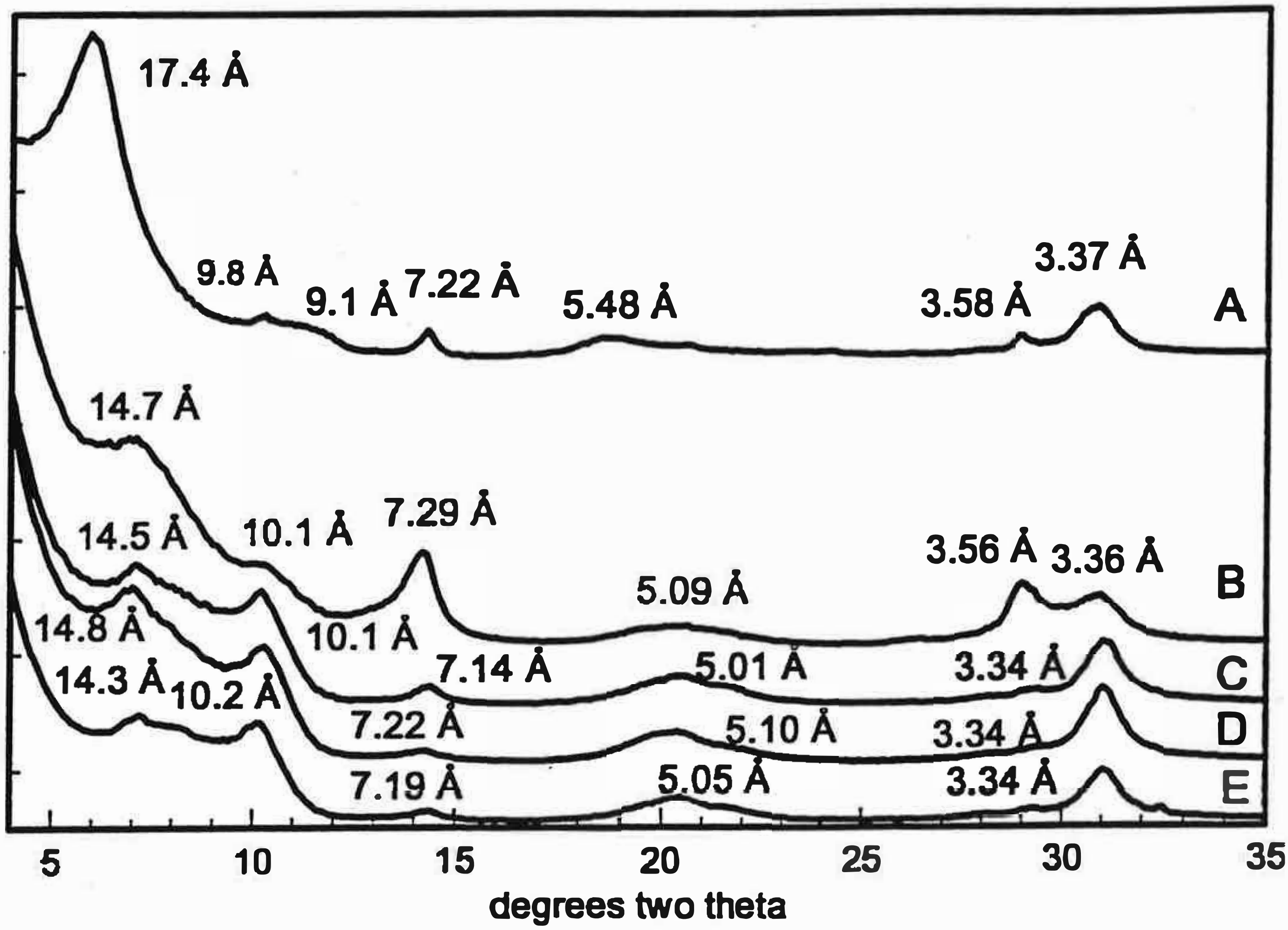

17.4 Å
9.8 Å
9.1 Å
7.22 Å
5.48 Å
3.58 Å
3.37 Å
A
14.7 Å
14.5 Å
10.1 Å
7.29 Å
3.56 Å
3.36 Å
B
5.09 Å
14.8 Å
10.1 Å
7.14 Å
5.01 Å
3.34 Å
C
14.3 Å
10.2 Å
7.22 Å
5.10 Å
3.34 Å
D
7.19 Å
5.05 Å
3.34 Å
E
5
10
15
20
25
30
35
degrees two theta

Fig. 5

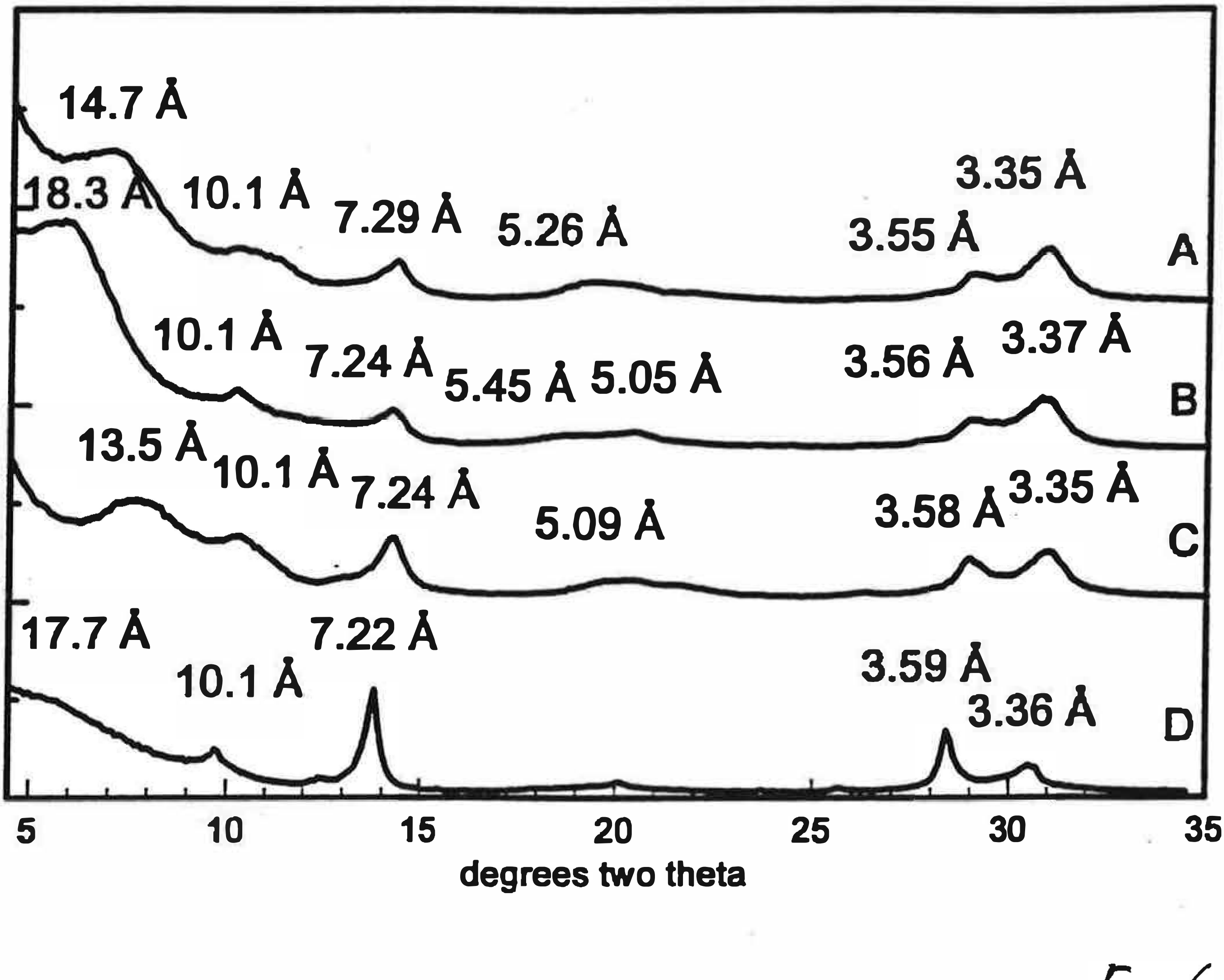

14.7 Å
18.3 Å
10.1 Å
7.29 Å
5.26 Å
3.35 Å
3.55 Å
A
10.1 Å
7.24 Å
5.45 Å
5.05 Å
3.56 Å
3.37 Å
B
13.5 Å
10.1 Å
7.24 Å
5.09 Å
3.58 Å
3.35 Å
C
17.7 Å
10.1 Å
7.22 Å
3.59 Å
3.36 Å
D
5
10
15
20
25
30
35
degrees two theta

Fig. 6

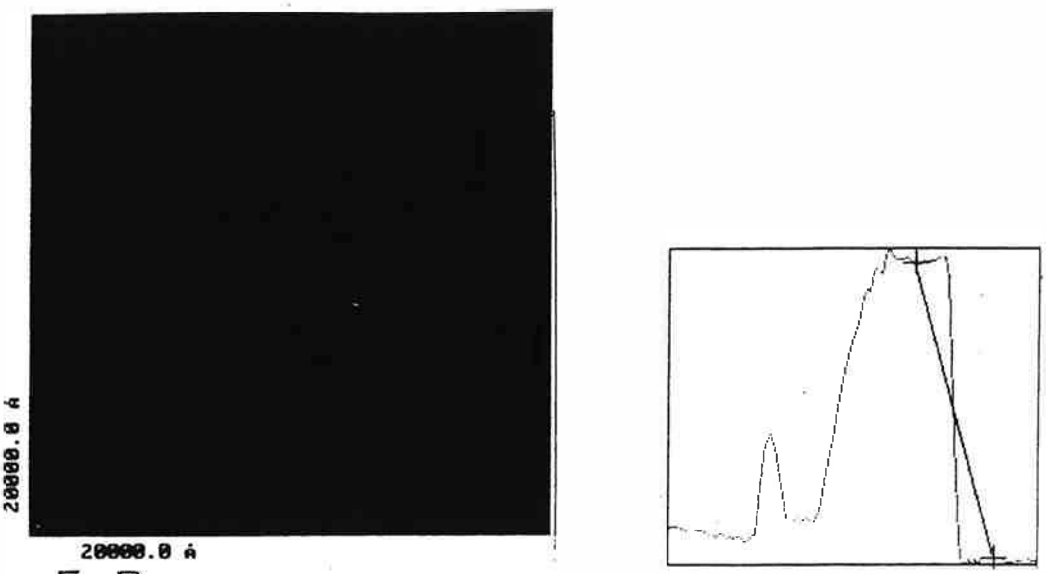

Fig. 7

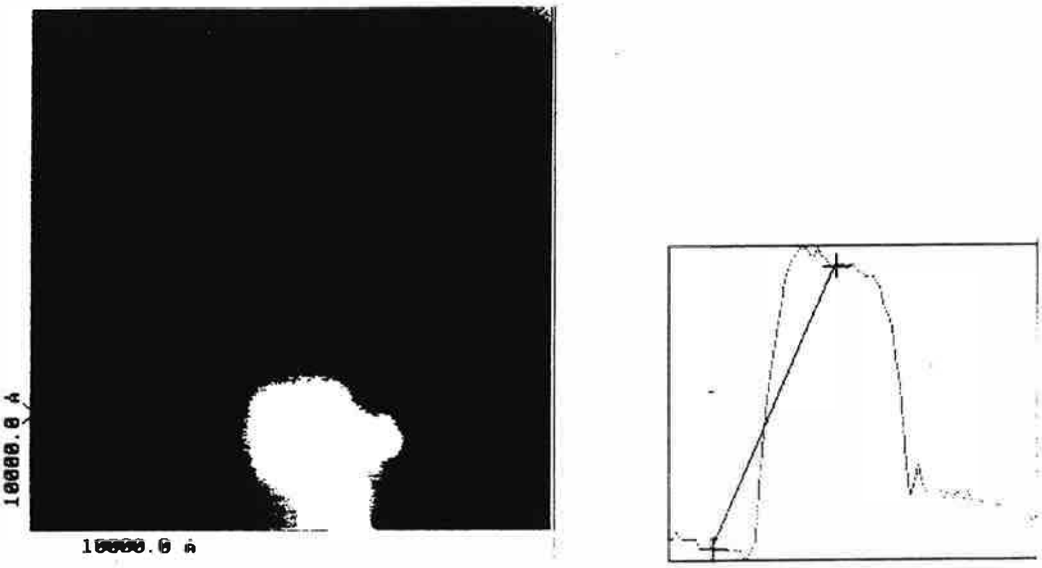

Fig. 8

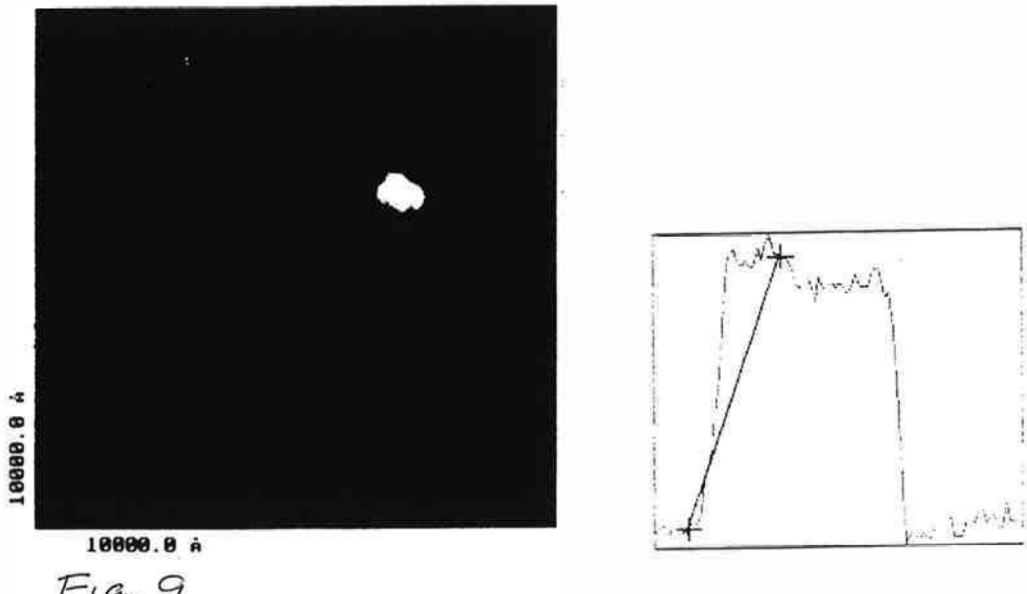

Fig. 9

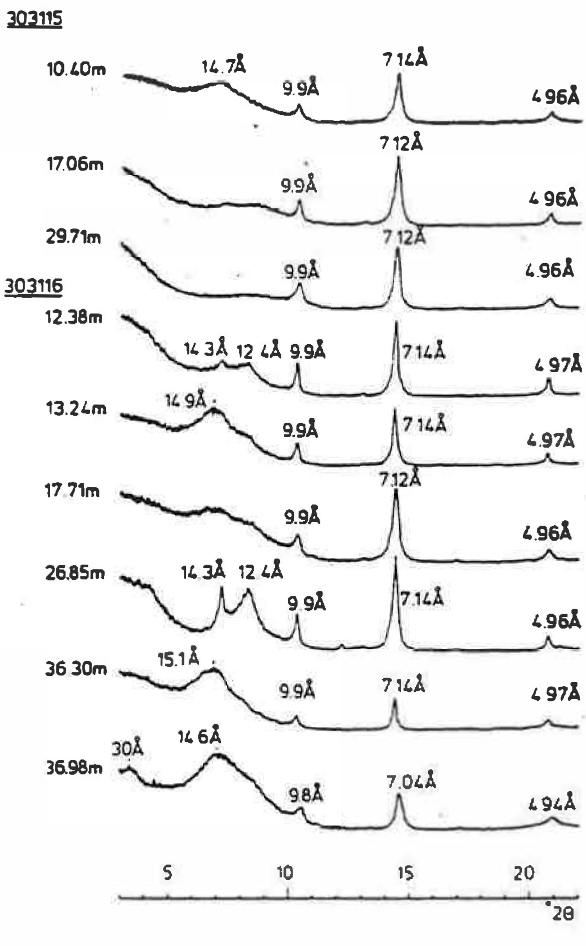

303115
10.40m
14.7Å
9.9Å
7.14Å
4.96Å
17.06m
7.12Å
9.9Å
4.96Å
29.71m
7.12Å
9.9Å
4.96Å
303116
12.38m
14.3Å
12.4Å
9.9Å
7.14Å
4.97Å
13.24m
14.9Å
9.9Å
7.14Å
4.97Å
17.71m
7.12Å
9.9Å
4.96Å
26.85m
14.3Å
12.4Å
9.9Å
7.14Å
4.96Å
36.30m
15.1Å
9.9Å
7.14Å
4.97Å
36.98m
30Å
14.6Å
9.8Å
7.04Å
4.94Å
5
10
15
20
°2θ

Fig. 10

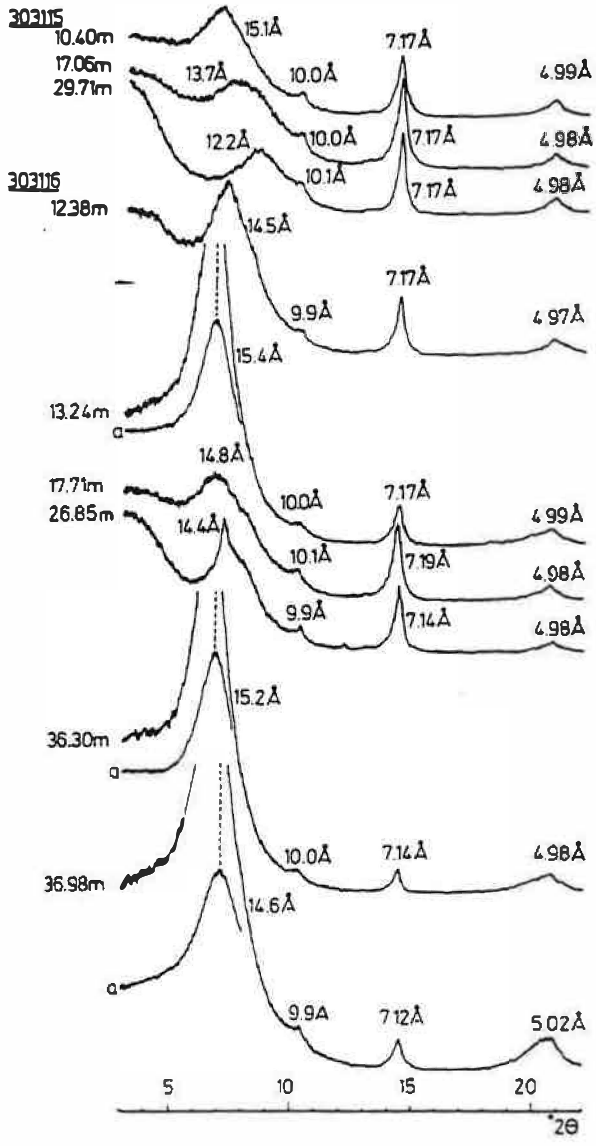
303115
10.40m
17.06m
29.71m
15.1Å
13.7Å
12.2Å
10.0Å
10.0Å
10.1Å
7.17Å
7.17Å
7.17Å
4.99Å
4.98Å
4.98Å
303116
12.38m
14.5Å
9.9Å
7.17Å
4.97Å
15.4Å
13.24m
a
14.8Å
17.71m
26.85m
14.4Å
10.0Å
10.1Å
9.9Å
7.17Å
7.19Å
7.14Å
4.99Å
4.98Å
4.98Å
15.2Å
36.30m
a
10.0Å
7.14Å
4.98Å
36.98m
14.6Å
a
9.9Å
7.12Å
5.02Å
5
10
15
20
°2θ

Fig. 11